Time-Domain Simulation of Rectangular Membrane Vibrations with 1-D Digital Waveguides

Forum Acusticum 2011 - Aalborg - Denmark

Time-Domain Simulation of Rectangular Membrane Vibrations with 1-D Digital Waveguides

Maarten van Walstijn and Eoin Mullan
Sonic Arts Research Centre, School of Electronics, Electrical Engineering, and Computer Science, Queen's University Belfast, United Kingdom.

Summary
One-dimensional musical resonators such as strings and tubes can be efficiently modeled in the time domain using digital waveguides. In this paper it is shown how 1-D digital waveguides may also be employed as efficient building blocks in simulations of higher dimensional systems governed by the wave equation. Focusing on synthesis of membrane vibrations driven by external forces, it is shown that all normal modes within a specified bandwidth can be captured with a finite set of extracted waveguides, each representing plane-wave motion in a specific direction. A digital realisation is presented and validated via numerical comparisons. The results of a computational complexity analysis indicate that - if a sufficient number of waveguides can be discarded - synthesis by digital waveguide extraction is more efficient than modal synthesis.

PACS no. 43.75.Zz, 43.75.Hi

1. Introduction

Sound synthesis by physical modelling relies largely on time-domain modelling of elemental vibrating structures, such as strings, tubes, bars, membranes, and plates. This paper addresses the simulation of the (linear) vibrations of a rectangular membrane driven by a point-force, as depicted schematically in 1(a). Membrane vibrations have been simulated with various modelling paradigms, including finite differences [1, 2], digital waveguide meshes [3, 4], and modal approaches [5, 6]. For 2-D problems, the computational complexity of these approaches is of the same order of magnitude, the operational count being proportional to the number of modes below Nyquist [1]. This contrasts with the simulation of the 1-D cousin of the membrane, the string, which - under specific simplifying assumptions - is simulated at much less computational cost with digital waveguides than with the other paradigms. The efficiency derives from the fact that, in its simplest form, a digital waveguide consists only of a pair of delay-lines that can be implemented as circular buffers at minimal cost using pointer arithmetic [7]. This benefit is lost in the 2-D version, since conventional arithmetic is required at each node of a digital waveguide mesh.

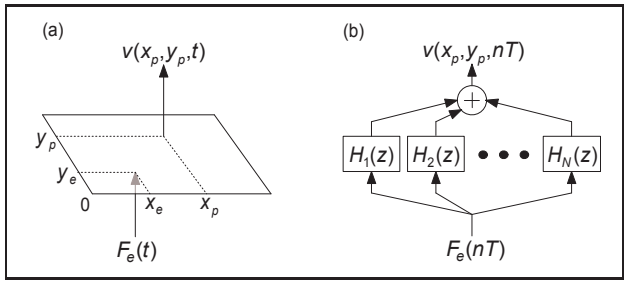

Figure 1. (a) Rectangular membrane driven by a force at position (x_e, y_e), while the velocity is observed at the coordinates (x_p, y_p). (b) Global structure of the digital waveguide extraction (DWE) model, which computes velocity at discrete-time instants $t = nT$, where T is the sampling period. Each block $H_q(z)$ respresents an extracted digital waveguide that simulates plane-wave motion in a specific direction.

In search of efficiency, various authors have found ways of reducing 2-D and 3-D wave motion to delay-line structures. Directly relevant to the current study is the synthesis method proposed by Aramaki [8], which consists of a parallel set of digital waveguides, each capturing a specific sub-group of normal modes. Another closely related study is that by Essl [9], who investigated how the motion of a circular membrane can be modeled - much like with geometrical methods - by iterating a fundamental solution. However, neither of these approaches led to improved membrane synthesis efficiency. Bilbao [10] showed that an initial

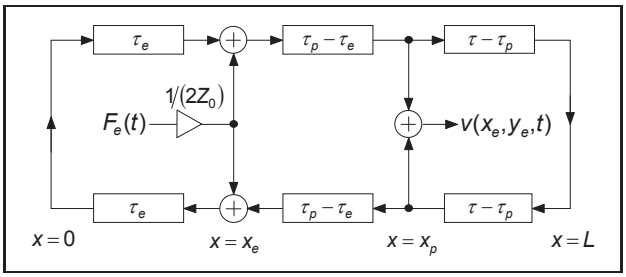

Figure 2. Waveguide model of an ideal string. An external force signal is applied at position $x = x_e$, and the velocity is observed at $x = x_p$.

value problem for an ideal square membrane with free boundary conditions can be solved by grouping modes into harmonic subsets, each of which can be simulated with a digital waveguide. The advantage compared to Aramaki's approach is that it does not involve large-order phase-adjusting loop filters, thus enabling greater efficiency. However it has not been detailed how to deal with external driving forces, propagation losses, non-square domains, and fixed boundary conditions.

This paper extends, refines, and re-evaluates the idea of synthesis via capturing harmonic subsets with digital waveguides, in application to rectangular membranes with free or fixed boundaries and driven by one or more external forces. The resulting digital waveguide extraction (DWE) model, which can be seen as a generalisation of Bilbao's approach, computes membrane velocities at discrete-time instants, and takes the form depicted in Fig. 1(b).

2. String Waveguide Model

The transversal motion of an ideal string driven by external forces is governed by [11]

$$w_{tt}(x,t) = c^2 w_{xx}(x,t) + (\rho A)^{-1} f(x,t), \qquad (1)$$

where w denotes string displacement, and $c = \sqrt{\mathcal{T}/(\rho A)}$ is the wave velocity that depends on tension ($\mathcal{T}$), mass density (ρ), and string cross-sectional area (A). Here w_{xx} and w_{tt} denote the second derivative of w with respect to the spatial coordinate (x) and time (t), respectively, and $f(x,t)$ denotes force density.

From the well-known D'Alembert solution to the wave equation, it follows that the velocity at any point is the sum of the forward- and backward travelling wave at that point. Assuming free boundaries (which is suited to the purposes of this study), an observation position x_p, and a driving force at a single position x_e, i.e. $F_e(t) = \int \delta(x - x_e) f(x,t) dx = f(x_e,t)$, the string may be modelled as depicted in Fig. 2. Each of the blocks represents the time it takes for a velocity wave to travel between two points on the string, and these delay values are expressed in terms of the time-delay parameters $\tau = L/c$, $\tau_e = x_e/c$, and $\tau_p = x_p/c$. This waveguide model can be thought of as the continuous model underpinning a digital waveguide string model [7], the driving source of which can be modeled by adding the signal $F_e(t)/(2Z_0)$ to the local velocity waves in both directions, where $Z_0 = \rho A c$ is the characteristic impedance.

From Fig. 2, the Laplace-domain transfer function of the string model can be deduced to be:

$$H(s) = \frac{\left(1 + re^{-2s\tau_e}\right)\left(1 + re^{-2s(\tau-\tau_p)}\right) e^{-s(\tau_p - \tau_e)}}{2Z_0(1 - r^2 e^{-2s\tau})}, \qquad (2)$$

and it can be shown - using Laplace and Fourier transforms - that the corresponding impulse response can be written

$$h(t) = \left(\frac{1}{2Z_0\tau}\right)\Big(2 + \sum_{m=1}^{\infty}\big\{\cos\left[\omega_m(t + \tau_e - \tau_p)\right] + \cos\left[\omega_m(t + \tau_e + \tau_p)\right] + \cos\left[\omega_m(t - \tau_e - \tau_p)\right] + \cos\left[\omega_m(t - \tau_e + \tau_p)\right]\big\}\Big). \qquad (3)$$

3. Modal Formulation of Membrane Response

Considering the spatial coordinates (x,y), the equation of motion for a lossless membrane driven by external forces is [11]

$$w_{tt}(x,y,t) = c^2 \Delta w(x,y,t) + (\rho b)^{-1} f(x,y,t), \qquad (4)$$

where the wave velocity $c = \sqrt{\mathcal{T}/(\rho b)}$ depends on the membrane tension per unit length ($\mathcal{T}$), the mass density (ρ), and the membrane thickness (b). Applying forced-motion analysis (see, e.g. [12]) and assuming fixed or free boundaries, the velocity response at pick-up position (x_p, y_p) to an impulse force applied at (x_e, y_e) can be derived and formulated in modal form as follows:

$$h(t) = \frac{\frac{1+r}{2} + \sum_{l=1}^{\infty}\sum_{m=1}^{\infty} W_{lm}(x_e,y_e) W_{lm}(x_p,y_p) h_{lm}(t)}{\frac{1}{4}\rho b L_x L_y} \qquad (5)$$

where $h_{lm}(t) = \cos(\omega_{lm} t)$ represents the reponse of a single mode indexed by (l,m), $W_{l,m}(x,y)$ is the mode shape function, and r denotes the boundary reflection coefficient. For fixed boundaries, we have $r = -1$ and

$$W_{lm}(x,y) = \sin(l\pi x/L_x)\sin(m\pi y/L_y), \qquad (6)$$

while for free boundaries, we have $r = 1$ and

$$W_{lm}(x,y) = \cos(l\pi x/L_x)\cos(m\pi y/L_y). \qquad (7)$$

For either boundary condition, the modal frequencies are

$$\omega_{lm} = \pi c \sqrt{\frac{l^2}{L_x^2} + \frac{m^2}{L_y^2}}. \qquad (8)$$

4. Waveguide Extraction

This section shows how the solution to the 2-D membrane problem can be decomposed into a set of 1-D waveguide solutions. The key notion is that the membrane motion can be considered as sum of plane wave motions:

$$h(t) = \sum_{q \in Q} h_q(t), \tag{9}$$

where Q is the collection of all possible directions. For investigating plane waves from a modal perspective, we consider a subset of (5) by setting

$$l = kq_x, \quad m = kq_y, \quad k = 1, 2, 3.... \tag{10}$$

where q_x and q_y are integers and $q = q_y/q_x$ represents the direction of wave travel. To avoid a direction being represented multiple times, q_x and q_y are restricted to mutually prime pairs [10]. Limiting ourselves to plane waves in one direction in a membrane with fixed edges then yields a subset impulse response function

$$h_q(t) = \frac{4}{\rho b L_x L_y} \sum_{k=1}^{\infty} W_k(x_e, y_e) W_k(x_p, y_p) \cos(\omega_k t), \tag{11}$$

with the normal modal shapes

$$W_k(x, y) = \sin(kq_x \pi x / L_x) \sin(kq_y \pi y / L_y), \tag{12}$$

and where the normal mode frequencies now form a harmonic subset:

$$\omega_k = \pi c \sqrt{\frac{k^2 q_x^2}{L_x^2} + \frac{k^2 q_y^2}{L_y^2}} = k \left(\frac{\pi c}{L_q} \right), \tag{13}$$

where $L_q = (L_x L_y) \,/\, \left(\sqrt{q_x^2 L_y^2 + q_y^2 L_x^2} \right)$. Note that we can also write

$$\frac{1}{L_x L_y} = \frac{\omega_k}{k \pi c \sqrt{q_x^2 L_y^2 + q_y^2 L_x^2}}. \tag{14}$$

Equation (12) can be written

$$W_k(x, y) = -\frac{1}{2} \Bigg\{ \cos \left[k\pi \left(\frac{q_x x L_y + q_y y L_x}{L_x L_y} \right) \right] - \cos \left[k\pi \left(\frac{q_x x L_y - q_y y L_x}{L_x L_y} \right) \right] \Bigg\}. \tag{15}$$

By substitution of (14) and then substituting the resulting equation into (11), it can be found that $h_q(t)$ can be written as follows:

$$h_q(t) = h_{e1,p1}(t) - [h_{e1,p2}(t) + h_{e2,p1}(t)] + h_{e2,p2}(t), \tag{16}$$

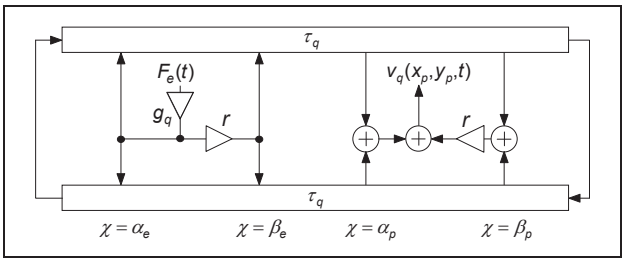

Figure 3. Waveguide system for modelling a plane-wave subset of the membrane response. The factor r represents the membrane boundary reflection coefficient, which is chosen as $r = -1$ for fixed boundaries and $r = 1$ for free boundaries.

where each of the four terms is of the form

$$h_{e,p}(t) = \frac{L_q}{2L_x L_y} \left(\frac{1}{2Z_0 \tau_q} \right) \sum_{k=1}^{\infty} \Big\{ \cos\left[\omega_k (t + \tau_e + \tau_p)\right] + \cos\left[\omega_k (t - \tau_e - \tau_p)\right] + \cos\left[\omega_k (t + \tau_e - \tau_p)\right] + \cos\left[\omega_k (t - \tau_e + \tau_p)\right] \Big\}, \tag{17}$$

and where $\tau_q = L_q/c$ and $Z_0 = \rho b c$ is the characteristic impedance of the membrane. Comparing (17) to (3) reveals that equation (17) equals the impulse response of a string with free boundaries and of length L_q, wave speed c, and characteristic impedance Z_0, but without the zero-frequency mode contribution, and with additional scaling by $L_q/(2L_x L_y)$. This means that in order to model the membrane with 1-D waveguides, we must replace the $1/(2Z_0)$ scaling factor as used in the waveguide string model (see Fig. 2) with

$$g_q = \frac{L_q}{2L_x L_y} \cdot \frac{1}{2Z_0} = \frac{L_q}{4Z_0 L_x L_y}. \tag{18}$$

In the sum of terms in (16), the zero-frequency mode contributions cancel each other out when each term is modelled as a 1-D waveguide string model.

Repeating the above derivations for free boundaries yields the same result, apart from the minus sign in (16), which becomes a plus sign. Hence a more general form is given in by

$$h_q(t) = h_{e1,p1}(t) + r\,[h_{e1,p2}(t) + h_{e2,p1}(t)] + h_{e2,p2}(t). \tag{19}$$

Since the four waveguide string models have the same effective length, the output for a plane-wave subset q may in fact be modeled using a single extracted waveguide model, in which the force signal is injected additively at two points along the system χ-axis,

$$\alpha_e = \frac{q_x x_e L_y + q_y y_e L_x}{\sqrt{q_x^2 L_y^2 + q_y^2 L_x^2}}, \; \beta_e = \frac{q_x x_e L_y - q_y y_e L_x}{\sqrt{q_x^2 L_y^2 + q_y^2 L_x^2}}, \tag{20}$$

and in which the output velocity is the sum of the values at extraction points

$$\alpha_p = \frac{q_x x_p L_y + q_y y_p L_x}{\sqrt{q_x^2 L_y^2 + q_y^2 L_x^2}}, \; \beta_p = \frac{q_x x_p L_y - q_y y_p L_x}{\sqrt{q_x^2 L_y^2 + q_y^2 L_x^2}}. \tag{21}$$

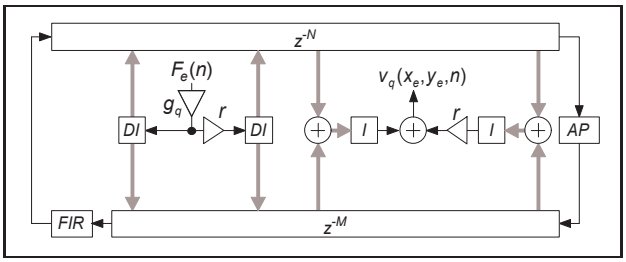

Figure 4. Digital realisation of a waveguide model for simulation of a plane-wave subset. The z^{-N} and z^{-M} blocks represent integer delay-lines, which are fractionally addressed using interpolation (I) and deinterpolation (DI) blocks. The multipliers with r merely allocate the sign (i.e. $r = \pm 1$) according to the specified membrane boundary conditions.

The block diagram for this arrangement is depicted in Fig. 3. As holds for an initial-value problem for a square membrane with free edges [10], the extracted-waveguide coordinates may take on values outside the range $[0, L_q]$, in which case they must be reflected into that range. A simple and numerically insensitive way to reflect the spatial coordinate χ to $\hat{\chi} \in [0, Lq]$ is

$$\hat{\chi} = \left(1 - \left|1 - \left(\frac{\chi}{L_q} \mod 2\right)\right|\right) L_q. \qquad (22)$$

5. Digital Realisation

The digital waveguide extraction (DWE) synthesis model takes the form of Fig. 1(b), i.e. a parallel set of 1-D digital waveguides. The discretisation of the extracted waveguides is performed following principles and techniques of the well-known digital waveguide modelling approach described in detail by Smith [7], which leads to the structure depicted in Fig. 4. The integer part of the time delay τ_q is realised with a digital delay-line of length $N = \lfloor L_q/(cT) \rfloor$, a Thiran all-pass (AP) filter is employed to model the sum $D = 2\,(L_q/(cT) - N)$ of the fractional parts of the lengths of the upper and lower delay-line. In order to simulate propagation losses, a linear-phase FIR filter [13] is used, although alternatively an IIR filter [14] can be employed. For maximum efficiency, the lowest possible filter orders are used here. That is, a first-order all-pass filter, which can be implemented with a single multiplier, is employed at the right-hand termination of Fig. 4, and a second-order FIR loss filter models the lumped propagation losses, which can be realised using just two multiplies. Since a second-order linear-phase FIR loss filter has a phase delay of exactly one sample, we may replace one of the unit delays of either the upper or lower delay-line with such a FIR section without affecting the overall loop delay time. For large membranes, cascaded FIR sections may occasionally be needed for the longer waveguides.

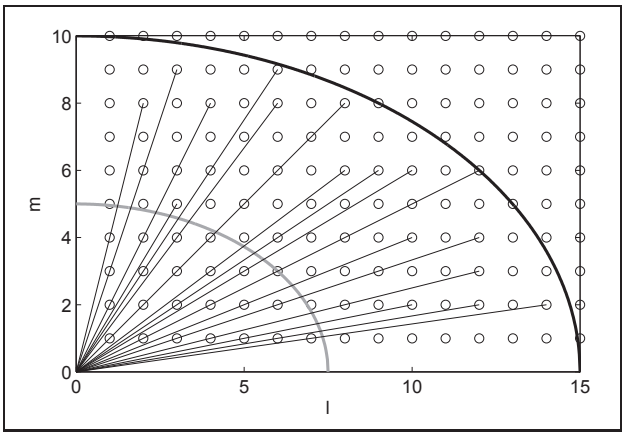

Figure 5. Modes represented as circles plotted at coordinates l, m. The thick black elliptic curve indicates the Nyquist limit, and the thick gray elliptic curve indicates the fidelity frequency f_ϵ limit. Each thin straight line represents a direction q, and the modes that it crosses are the modes captured by the digital waveguide q.

As shown in Fig. 4, the digital input signal $g_q F_e(n)$ is injected into the upper and lower delay-line using deinterpolators (DI), and the velocity output signal $v_q(x_p, y_p, n)$ is extracted from the delay-lines by means of linear interpolator (I) blocks. The use and design of interpolators and deinterpolators in the context of digital waveguide modelling is described in detail by Välimäki [15]. Here linear (de)interpolators are used, i.e. first-order Lagrange FIR filters, which can be realised using a single multiplier.

6. Reduced DWE Model

Musical sounds and other audio signals usually have a large part of their energy in the low-frequency range, and therefore it is worth considering a fidelity frequency $f_\epsilon \leq 0.5 f_s$ above which accuracy is traded off against efficiency, the underlying hypothesis being that this frequency can be chosen so that no or little significant perceptual change is affected [10]. Computational savings are then made by only including digital waveguides that have a fundamental lower than f_ϵ, which leads to a reduced, less costly DWE model. As an example, Fig. 5 demonstrates the modes that are captured by a reduced DWE model ($f_\epsilon = 0.25 f_s$) in the case of a rectangular membrane ($L_x = 7.5X$, $L_y = 5X$) with fixed boundaries. Note that all modes with frequencies below the f_ϵ limit are captured, but that the DWE model naturally also produces a number of modes above f_ϵ. In other words, some high-frequency detail always remains.

7. Multiple Outputs and Inputs

In audio applications of the membrane model, it is often desirable to work with multiple inputs and out-

(c) European Acoustics Association, ISBN: 978-84-694-1520-7, ISSN: 221-3767

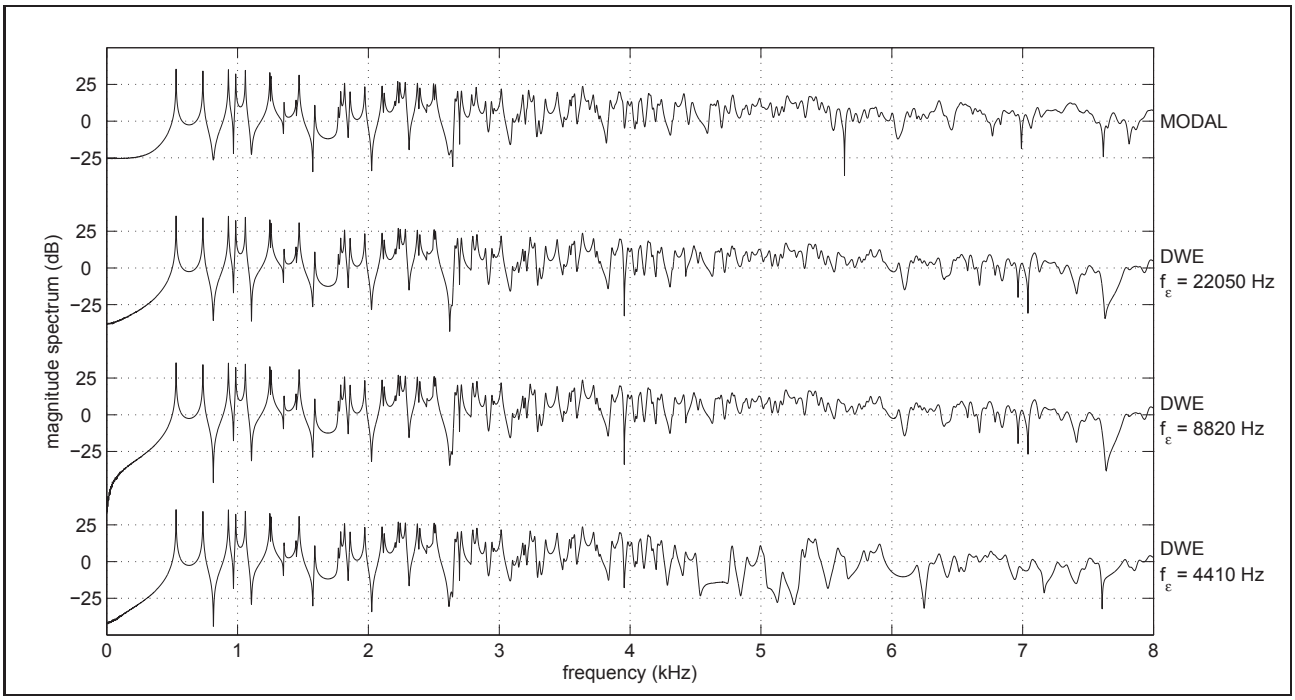

Figure 6. Spectra of the output velocity signals, calculated for the membrane parameters $\rho = 100\,\mathrm{Kg\,m^{-3}}$, $b = 1.0\,\mathrm{mm}$, $L_x = 120.26\,\mathrm{mm}$, $L_y = 18.17\,\mathrm{mm}$, $\mathcal{T} = 500\,\mathrm{N\,m^{-1}}$, $b_1 = 3\,\mathrm{s^{-1}}$, $b_2 = 0.0003\,\mathrm{m^2\,s^{-1}}$, $x_e = 24.05\,\mathrm{mm}$, $y_e = 24.05\,\mathrm{mm}$, $x_p = 72.15\,\mathrm{mm}$, $y_p = 56.12\,\mathrm{mm}$.

puts. This requires that for N_{in} inputs and N_{out} membrane outputs, each digital waveguide has $2N_{in}$ injection points and $2N_{out}$ extraction points. Regarding modal synthesis, a realisation with multiple inputs and outputs requires, as with the functional transformation method [5], N_{in} coefficients at the input side and N_{out} coefficients at the output side. This leads to $(N_{in} + N_{out})$ coefficients per mode, in addition to two coefficients per (lossy) oscillator.

8. Numerical Results

In order to investigate the validity of the DWE model and to inspect the degradation of the output signal when the model captures a reduced set of modes, the output velocity of a fixed-boundary membrane was calculated, using a short Gaussian pulse force input signal. This calculation was performed with the full modal model and with three DWE models, using the fidelity frequencies $f_\epsilon = 0.5 f_s$, $f_\epsilon = 0.2 f_s$, and $f_\epsilon = 0.1 f_s$. All models used a sampling frequency $f_s = 44100\mathrm{Hz}$. The resulting magnitude spectra, shown in Fig. 6, confirm that a decrease in f_ϵ results in a reduction of the bandwidth in which the modal and the DWE model produce a similar spectrum.

9. Computational Complexity

In analysing the computational complexity, the number of runtime multiplies required is taken as the criterion to base any complexity measures on, and a scenario with N_{in} inputs and N_{out} outputs is assumed. A further assumption is that the loss filter requires two multiplies, thus any small additional cost that may occur when employing the cascaded FIR design for large membranes with strong losses is neglected. In the DWE model, the number of multiplies per digital waveguide is $M_{dwg} = 4 + 2\,(N_{in} + N_{out})$, while in the modal model, the number of multiplies per mode is $M_{mod} = 2 + N_{in} + N_{out}$. It can be shown that the number of digital waveguides required to capture all modes of frequency less than f_ϵ is approximately $N_{dwg} \approx \left(6 f_\epsilon^2 S / \left(\pi c^2\right)\right.$, where $S = L_x L_y$ is the membrane surface area. The total number of modes generated by these N_{dwg} digital waveguides is approximately $N_{mod} \approx (2 f_s / c)\,\sqrt{\eta N_{dwg} S}$ where $\eta = 1/3$ for fixed boundaries and $\eta = 2/5$ for free boundaries. The output generated by the DWE model with fidelity up to f_ϵ could also be calculated with a reduced modal model in which the same set of modes is captured. Hence the *relative computational complexity* of the DWE model may be seen as the ratio of total number of multiplies needed to render that output:

$$R = \frac{N_{dwg} M_{dwg}}{N_{mod} M_{mod}} = \sqrt{\frac{6}{\eta\pi}} \left(\frac{f_\epsilon}{f_s}\right). \tag{23}$$

In order to estimate the overall reduction in complexity, we define a second complexity measure, $\bar{R}$, that compares the reduced DWE model to a full

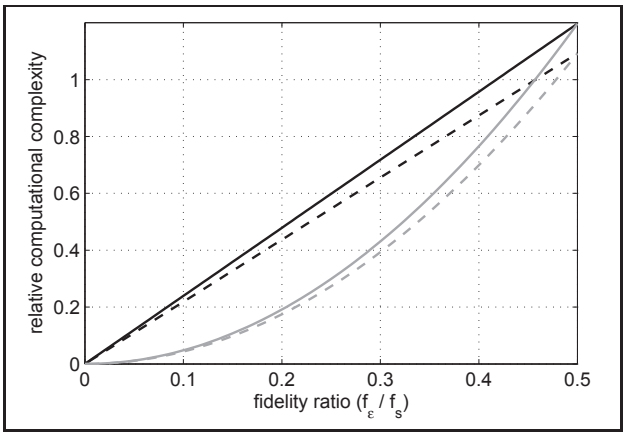

Figure 7. Relative computational complexity ratios R (black lines) and $\bar{R}$ (gray lines) for fixed boundaries (solid) and free boundaries (dashed).

modal model (that captures all $\bar{N}_{mod}$ modes below Nyquist):

$$\bar{R} = \frac{N_{dwg} M_{dwg}}{\bar{N}_{mod} M_{mod}} = 2\sqrt{\frac{6}{\eta\pi}} \left(\frac{f_\epsilon}{f_s}\right)^2 . \qquad (24)$$

Fig. 7 shows R and $\bar{R}$ as a function of f_ϵ/f_s. From the R plots it can be seen that the DWE model is more efficient than a modal model that generates the same sound as long as the fidelity ratio f_ϵ/f_s is less than around 0.42, and that the associated complexity reduction is around 40% for $f_\epsilon/f_s = 0.25$. The $\bar{R}$ plots indicate that the overall reduction in complexity is about 70% for $f_\epsilon/f_s = 0.25$.

10. Concluding Remarks

We have shown how membrane vibrations may be modeled and digitally synthesised as the sum of the outputs of a set of extracted digital waveguides, each representing plane-wave motion in a specific direction. The computational complexity of the model - defined here as the total number of required multiplies - may be reduced by only including digital waveguides of a fundamental frequency less than a chosen fidelity frequency (f_ϵ), and thus capturing fewer system modes, at the cost of decreased accuracy. Our comparisons have indicated that for fidelity frequencies smaller than about 84% of the Nyquist frequency, the DWE modelling approach affords greater complexity reductions of this kind than a modal approach that discards the same number of modes.

A question that naturally arises from these findings is how small one may choose f_ϵ before any perceptual difference occurs. Preliminary listening tests using a 44.1kHz sample rate have indicated that, in general, no difference is perceivable if f_ϵ is at least about half of the Nyquist frequency. This means that - compared to a full modal model - an overall reduction in computational complexity of 70% can be made.

A further question that could be addressed by future research is whether the principle of using 1-D waveguides to model higher-dimensional systems can also be applied to objects of different characteristics or geometry.

References

[1] Stefan Bilbao, *Numerical Sound Synthesis*, John Wiley & Sons, Chichester, 2009, Chap. 11.

[2] M. van Walstijn and K. Kowalzyk, "On the numerical solution of the 2-D wave equation with compact FDTD schemes," in *Proc. 11th International Conference on Digital Audio Effects (DAFX08)*, Espoo, Finland, 2008, pp. 205–212.

[3] S. A. van Duyne and J. O. Smith, "Physical modeling with the 2-D digital waveguide mesh," in *Proc. International Computer Music Conference*, Tokyo, 1993, pp. 40–47.

[4] L. Savioja and V. Välimäki, "Interpolated rectangular 3-D digital waveguide mesh algorithms with frequency warping," *IEEE Trans. Speech Audio Process*, vol. 11, no. 6, pp. 783–790, Nov 2003.

[5] L. Trautmann and R. Rabenstein, *Digital Sound Synthesis by Physical Modelling Using the Functional Transformation Method*, Kluwer Academic/Plenum Publishers, New York, 2003, pp. 1-226.

[6] F. Avanzini and R. Marogna, "A modular physically-based approach to the sound synthesis of membrane percussion instruments," *IEEE Trans. Audio Speech Lang. Processing*, vol. 18, no. 4, pp. 891–902, Apr 2010.

[7] J. O. Smith, *Physical Audio Signal Processing*, Stanford University, `http://ccrma.stanford.edu/~jos/pasp/`, online book, date last viewed 10/12/2010.

[8] M. Aramaki, *Analyze-synthese de sons impulsifs: Approches physique et perceptive*, Ph.D. thesis, Univ. Mediterrannee-Aix Marseille II, Marseille, France, 2002.

[9] G. Essl, "Iterated fundamental solution simulations of sections of circular membranes," in *Proc. International Symposium for Musical Acoustics (ISMA)*, Barcelona, 2007.

[10] S. Bilbao, "Fast modal synthesis by digital waveguide extraction," *IEEE Signal Processing Letters*, vol. 13, no. 1, pp. 1–4, jan. 2006.

[11] N. Fletcher and T. Rossing, *The Physics of Musical Instruments*, Springer, New York, 1998, 2nd edition.

[12] Karl F. Graff, *Wave Motion in Elastic Solids*, Dover Publications, New York, 1991, 2nd edition, Chap. 1.

[13] Maarten van Walstijn, "Parametric FIR design of propagation loss filters in digital waveguide string models," *IEEE Signal Processing Letters*, vol. 17, pp. 795–798, 2010.

[14] B. Bank, "Physics-based sound synthesis of the piano," M.S. thesis, Budapest Univ. Technol. and Economics, Budapest, Hungary, 2000, Report 54, Helsinki Univ. of Technology, Lab. of Acoustics and Audio Signal Processing.

[15] V. Välimäki, *Discrete-Time Modeling of Acoustic Tubes Using Fractional Delay Filters*, Ph.D. thesis, Helsinki University of Technology, Finland, 1995.